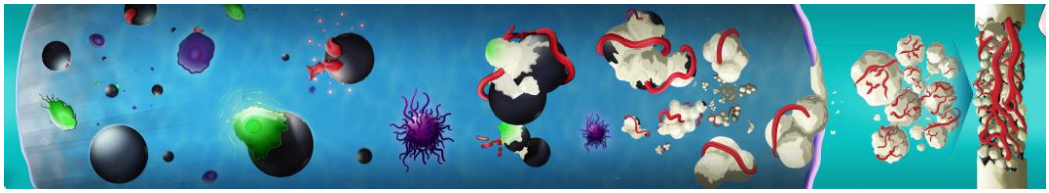

COMPASS

ENGINEERING LIFE GUIDED BY NATURE

This paper must be cited as: Vilabril, S., Nadine, S., Neves, C. M., Correia, C. R., Freire, M. G., Coutinho, J. A., Oliveira, M. B., & Mano, J. F. One-Step All-Aqueous Interfacial Assembly of Robust Membranes for Long-Term Encapsulation and Culture of Adherent Stem/Stromal Cells. 10(10), 2100266. Advanced Healthcare Materials, (2021). https://doi.org/https://dx.doi.org/10.1002/adhm.202100266

One-step All-aqueous Interfacial Assembly of Robust Membranes for Long-term Encapsulation and Culture of Adherent Stem/Stromal Cells

Sara Vilabril, Sara Nadine, Catarina M. S. S. Neves, Clara R. Correia, Mara G. Freire, João A. P. Coutinho, Mariana B. Oliveira, João F. Mano**

S. Vilabril, S. Nadine, Dr. C. M. S. S. Neves, Dr. C. R. Correia, Dr. M. G. Freire, Prof. J. A. P. Coutinho, Dr. M. B. Oliveira, Prof. J. F. Mano

CICECO – Aveiro Institute of Materials, Department of Chemistry, University of Aveiro, 3810-193, Aveiro, Portugal.

E-mail: mboliveira@ua.pt (M. B. Oliveira); jmano@ua.pt (João F. Mano)

Keywords: all-aqueous fabrication, cell-laden capsules, interfacial complexation, aqueous two-phase systems

The therapeutic effectiveness and biological relevance of technologies based on adherent cells depend on platforms that enable long-term culture in controlled environments. Liquid-core capsules have been suggested as semi-permeable moieties with spatial homogeneity due to the high mobility of all components in their core. The lack of cell-adhesive sites in rapidly formed liquid-core structures often hampers their use as platforms for stem cell-based technologies for long-term survival, multilineage differentiation and cell-directed self-organization. Here, the one-step fast formation of robust polymeric capsules formed by interfacial complexation of oppositely charged polyelectrolytes in an all-aqueous environment, compatible with the encapsulation of mesenchymal stem/stromal cells (MSCs) and microcarriers, is described. Encapsulated umbilical cord MSCs adhered to polymeric microcarriers and proliferated for more than 21 days in capsules prepared either manually by drop-wise addition, or by scalable electrohydrodynamic atomization. The system was cultured under static or dynamic (bioreactor) environment, showcasing its robustness, stability, and versatility.

1. Introduction

The use of extracellular matrix (ECM)-mimetic bulk hydrogels has led to major advances on the exploration of the use of stem cells for tissue regeneration and *in vitro* organ fabrication.[1] These three-dimensional (3D) polymer-based structures are usually flexible, transparent, rich in water, and easily tailored, both chemically and mechanically.[2] However, some major drawbacks associated with these structures are related with the lack of spatial freedom for cells to proliferate and migrate in order to create an organized tissue, and with the low diffusion capacity of essential molecules to these structures' core, compromising the proper biological function of encapsulated living cells over the whole depth of the biomaterial construct.[3] Semipermeable capsule-shaped membranes comprising a liquid core simultaneously allow the confinement of biological cargo, while enabling the diffusion of nutrients and essential molecules, such oxygen (O_2) and carbon dioxide (CO_2). The first remarkable application of liquid-core capsules for cellular therapies was reported by Lim and Sum, targeting the immune isolation of pancreatic islets for transplantation of diabetic individuals.[4] Most methods described to produce liquid-core capsules rely either on the primary production of beads, often obtained by gelation, or in the use of oil-based emulsion/templating techniques. Gelled beads are used as sacrificial templates that support the formation of a limitative membrane, often by the deposition of antagonistic molecules.[5] Reactions driving the formation of these membranes usually occur either by complexation or precipitation of oppositely charged polyelectrolytes[6] and/or nanoparticles,[7] or by their layer-by-layer (LbL) deposition.[8] The removal of (semi-)solid sacrificial templates is achieved in a sequential post-processing step, and often requires the use of organic solvents, [9–11] ionic chelating agents,[12] or temperature cycles,[13] giving rise to multi-step, complex and time-consuming processes. Oil-based methodologies also rely on the formation of oil droplets to

sustain the formation of membranes, showing detrimental effects on the biological cargo and difficult clinical translation.[14,15]

In the mid-1950s, aqueous two-phase systems (ATPS) were presented as a biocompatible alternative for liquid-liquid extraction techniques capable of competing with traditional methodologies that often involve volatile organic solvents.[16] ATPS are characterized by a mixture of two incompatible hydrophilic materials – which may be two polymers, or a polymer and a salt - on aqueous solution. Depending on the concentration of the components, the systems may separate into two immiscible aqueous phases.[17] With the increasing need for safer and easier strategies to facilitate the encapsulation of molecules and biological cargo, ATPS emerged as a simple, versatile and viable solution to produce a large variety of structures.[18] ATPS' phases have been enriched with reacting molecules to promote interfacial reactions. In this context, the complexation of polyelectrolytes/nanoparticles[19] and polyelectrolyte/polyelectrolyte[20] pairs were used to fabricate liquid-core capsules with permeable tailored membranes. The concept was materialized through the exploration of different techniques, including microfluidics[21,22] and electrospraying,[23,24] culminating in the formation of multiscale structures. So far, biocompatible encapsulation devices fabricated using ATPS as all-aqueous emulsion supports has been restricted to scenarios where cells were grown in suspension conditions. While the studies by Weitz[25] and Lee[26] refer to the encapsulation of bacteria, a recent study by Qin and coworkers[27] showed that multicellular islet organoids (multicellular aggregates) could be assembled in complexed alginate/chitosan membranes.

Despite the value of liquified capsules as tools to promote the formation multicellular aggregates, the long-term survival of adherent cells, namely clinically relevant mesenchymal stem cells (MSCs), is dependent on the provision of adhesion sites. The lack of ECM-mimetic cell-adhesive cues either directs cells into the formation of multicellular aggregates that tend to show poor diffusion properties, generating necrotic cores upon prolonged times of

culture[28] or, upon insufficient establishment of cell contact to guide aggregates' formation, individual cells tend to die from anoikis.[29] Correia *et al*. previously suggested the incorporation of polymeric microparticles inside liquified capsules made by the layer-by-layer technique, followed by the retrieval of sacrificial template, as an effective method to enable the adhesion, proliferation and modulation of adipose-derived mesenchymal stem cells for cell differentiation.[30,31]

Here, we propose a rapid one-step oil-free encapsulation method to generate a robust and permeable membrane with the shape of closed capsules. Phases of the well-described poly(ethylene glycol) (PEG)/dextran (Dex) ATPS were mixed with oppositely charged polyelectrolytes ε-poly-L-lysine (PLL) and alginate (ALG), respectively. Polyelectrolyte complexation promoted at the interface of the ATPS enabled the generation of insoluble and stable membranes using a dropwise pouring method to create millimetric capsules, and electrohydrodynamic atomization (EHDA) to form micrometric structures. The simultaneous encapsulation of animal cells – L929 immortalized mouse lung fibroblast cell line or human umbilical cord mesenchymal stem/stromal cells (hUC-MSC) – along with poly(ε-caprolactone) microcarriers enabled attaining high cellular viability up to 21 days after encapsulation, both in static or dynamic culture regimens. The versatile system may be adapted to additional polymeric combinations and used to compartmentalize sensitive cargo in various fields, including drug delivery, environmental applications, or food development.

2. Results

2.1. Liquid-core capsules are formed within the interface of all-aqueous immiscible phases

The formation of ALG/PLL hybrid capsules at the interface of the all-aqueous immiscible system was initially explored through the observation of the system's visual features after a simple Phase I-in-Phase II drop-wise addition strategy **(Figure 1A,B)** and, later on, by a

scalable EHDA technique **(Figure 1C)**. The transparent character of both initially separated solutions enabled the detection of the formation of an opaque interfacial membrane after the addition of the disperse ALG-loaded Phase I into the continuous PLL-loaded Phase II.

The formation of a stable membrane at the droplet's interface that separates both aqueous immiscible phases was expected to be mainly ascribed to electrostatic interactions, at pH 7.4, of positively charged PLL (reported pK_a ~9-10 [32]), and negatively charged ALG (reported pK_a ~3-4 [33]). Previous studies based on the layer-by-layer technology show that the two polymers are capable of interacting, forming insoluble films.[8,34] The charge of each molecule was assessed in two different solutions: with the polyelectrolytes dissolved in DPBS, or in the corresponding ATPS' phase, both after a pH adjustment to physiologic value (7.4). While in DPBS PLL showed a net charge of +7.91 ± 1.8 mV and ALG of -57.80 ± 5.53 mV, the addition of the ATPS' components (Dex, for ALG; PEG, for PLL) led to a significant decrease in the modular values of the net charge previously detected for each phase. PEG+PLL exhibited a net charge close to neutral of +0.98 ± 0.3 mV and the Dex+ALG solution followed the same trend, with a value of -4.99 ± 0.56 mV, which may be explained by the shielding effect of uncharged ATPS-composing polymers on charged polymers.[35,36] Phase II (PEG+PLL) showed much lower viscosity than Phase I (Dex+ALG) and both phases showed shear-thinning behavior **(Figure S1)**. These properties probably favored the easy drop-wise addition of Phase I into Phase II, while enabling the formation of a continuous phase with extremely low viscosity under agitation, important to ensure physical distancing between formed capsules and to avoid their clumping during complexation.

Millimetric capsules with an average diameter of 2.78 ± 0.10 mm were obtained using alginate (1.5% (w/w)) and PLL (0.5% (w/w)) complexed for 15 minutes. Membrane's analysis right after production allowed estimating a thickness of 132 ± 12 µm. Those membranes were resistant to a dynamic environment of DPBS under agitation, as well as to their contact with air **(Figure 1D)**. Electrosprayed capsules processed using alginate (1%

(w/w)) and PLL (0.5% (w/w)) showed a smaller diameter of 767.2 ± 85.3 µm. Both macro- and microcapsules showed extensive hollow cores and continuous membranes with smooth outer surface and cross-sectional microporosity **(Figure 1E)**.

2.2. Capsules show mechanical robustness, permeability, and amenability to integrate hierarchical structures

To explore the versatility of the developed system, we tested an array of different concentrations of the polyelectrolyte's pair as well as different complexation times. **Figure 2A** summarizes the robustness' features of macrocapsules complexed for 20 minutes using three concentrations of alginate [ALG] wt% = 0.5%, 1%, or 1.5% and three concentrations of polylysine [PLL] wt% = 0.5%, 1%, or 1.5%. Three out of the nine formulations yielded robust capsules, amenable to be easily handled: 1.5wt% ALG + 0.5 wt% PLL, 1.5 wt% ALG + 1 wt% PLL and 1.5 wt% ALG + 1.5 wt% PLL. Interestingly, capsules prepared with the lowest PLL concentration showed higher resistance to centrifugation cycles up to 769 g **(Figure 2B)**. Moreover, with the adaptation of the system for cell encapsulation in mind, that condition was selected for further characterization, since exposure to high concentrations of PLL has been reported as toxic[37,38] The possibility of reducing the complexation time was then assessed. Times of complexation below 10 minutes led to the formation of fragile capsules, unamenable to withstand contact with air or washing steps with DPBS. Upon centrifugation cycles, lower complexation times correlated with increasing rates of disrupted membranes **(Figure 2C)**: with 20 minutes of complexation, approximately 20% of the structures ruptured, increasing to 80% for a complexation time of 10 minutes. An intermediate point - 15 minutes of complexation - ensured the rapid production of capsules with robust behavior and, consequently, this condition was selected for further experiments.

The mechanical resistance of the capsules with both size ranges was evidenced through the efficient encapsulation of micro- in macro-capsules **(Figure 2D, Movie S1)**, giving rise to an easy methodology to generate multi-scale compartmentalized structures. This approach may enable the creation of complexly designed multi-core devices to incorporate different cells and essential biomolecules, allowing a regulated coexistence in physically protected and semipermeable environments, not compromising the individual integrity and proper function of each individual system. This may be adapted either to mimic the intracellular environment of living cells within organelles, or for tissue engineering by taking advantage of important co-cultures and essential regulatory signaling pathways.[39]

The permeability of 1.5% ALG + 0.5% PLL macrocapsules was assessed by the release of dextrans-FITC with molecular weights ranging from 10 kDa to 500 kDa. Release profiles obtained until 28 hours of incubation suggest that capsules are permeable to linear molecules with a molecular weight of 150 kDa, although slower release profiles were observed with increasing the molecular weights of the dextran-FITC **(Figure 2E)**. Molecules with 500 kDa showed a total release of ~20% of initially loaded mass, probably corresponding to entrapped molecules in superficial regions of the capsules, since this release was rapidly stabilized indicating that only a low portion of these molecules could diffuse from the capsules. Interestingly, the release profile for all molecules reached a plateau-like stage after short incubation times, around 200 minutes. The rapid diffusion of the smallest molecular weight molecule (10 kDa) suggests that capsules are easily permeable to low molecular weight compounds essential for cell survival, including oxygen, nutrients, and cell's metabolic waste.

2.3. Capsules prepared in all-aqueous medium enable the loading of microcarriers and the long-term viability of encapsulated adherent cells

We demonstrated the ability to encapsulate model molecules in mild conditions concerning pH, temperature, agitation, and time. The adequacy of the developed encapsulation method to withstand human cells' encapsulation was further tested with adherent cells. With the aim of providing necessary adhesion sites for cell attachment, plasma-treated PCL microcarriers were simultaneously encapsulated with cells, in a one-step procedure. A well-accepted fibroblast immortalized cell line recurrently used to study biomaterials' cytotoxicity[40–42] survived the encapsulation procedure and proliferated while cultured in the core of the macrocapsules for 21 days **(Figure S2-A)**. Those cells – L929 – seemed to first form cell-cell aggregates and only around 7 days in culture started attaching to the PCL microcarriers, increasing their proliferative behavior and metabolic activity **(Figure S2-B)**, forming cellular aggregates up to 21 days in culture. Both cells and microcarriers were effectively encapsulated inside the complexed ALG/PLL membrane and non-encapsulated cells could not be found outside the capsule's walls.

The encapsulation of human primary stem/stromal cells with clinical relevance[43–47] was then assessed using hUC-MSCs. Viable cells were detected after 1 day in culture, both under static and dynamic (rotational bioreactor) regimens **(Figure 3A)**. Moreover, hUC-MSCs adhered to plasma-treated and type I collagen-coated microcarriers at this early time point. Dynamic culture seemed to promote **(Figure 3B, Movie S2)** an effective cell attachment to microcarriers, where a boost in the formation of cellular aggregates and proliferative behavior were observed in this condition up to 21 days of cell culture. These results were corroborated by the increase in the cellular metabolic activity (normalized by total dsDNA) **(Figure 3C)** observed for bioreactor-cultured cells. Encapsulated hUC-MSCs in static culture conditions tended to form micrometric aggregates mediated by multiple cell-microparticles contacts after 40 days in culture, which apparently adhered to the capsules' inner wall, leading to their rupture after 57 days in culture **(Figure S3)**. With the increasing growth of those cell-microcarriers aggregates, the generated tension on the capsules' membrane probably led to

their localized rupture, allowing aggregates to escape from the capsules without the loss of their spherical structure.

Microcapsules also enabled the encapsulation of hUC-MSCs with efficacy and keeping high cellular viability.[48,49] The live/dead assay was performed on encapsulated hUC-MSC for 1, 3, 7 and 14 days in culture. Likewise, as observed in macrocapsules, encapsulated PCL microcarriers showcased attached cells and, upon cellular proliferation, those structures evolved into microaggregates, after one week in culture **(Figure 3D)**. Capsules' diameter of 526±74 μm were obtained, showing a significant reduction in size when compared to cargo-less microcapsules.

3. Discussion

The design of new encapsulation strategies capable of surpassing current hurdles associated with conventional 3D single-phase hydrogels may facilitate and accelerate the clinical translation of cellular therapies. While cell encapsulation in liquid-core capsules seems to fulfill several requirements to outperform materials with bulk structures,[3,30] developing technologies compatible with their safe, scalable, one-step and rapid production are still in great demand. Most technologies that aim at producing liquid capsules still rely either (i) on the use of oil or other organic agents, difficult to remove during washing cycles with aqueous solvents and frequently associated with cytotoxicity, or (ii) on the use of sacrificial templates to deposit conformal coatings, requiring multi-step processing procedures, as well as the use of additional components that may impart the hybrid biologic systems with unpredictable behavior. Additionally, the incorporation of cell-adhesive microparticles in the core of liquified capsules - necessary to generate a favorable environment for adherent cells - has been restricted to LbL capsule's formation technologies, followed by chelating steps to promote cores' liquefaction.[12,30,50]

In this study, we hypothesized that the encapsulation and long-term cell culture of clinically relevant human mesenchymal stromal cells[46,47] and solid microcarriers could be attained in a one-step all-aqueous procedure. The system would take advantage of the well-reported phase-separation's properties of ATPS, as well as from their ability to promote an interfacial complexation of oppositely charged polyelectrolytes. Although the encapsulation of biological cargo, namely bacteria and animal cells, has been reported using similar concepts,[25–27] it was not clear whether the encapsulation of polymeric microparticles would be feasible using these systems and if the majority of the cargo would be entrapped in the capsules' liquid core. We showed that both cells and microparticles could be efficiently encapsulated and kept in the liquid core of capsules prepared with ALG and PLL, at physiologic pH and ionic strength, as well as at room temperature. The compatibility of the developed system with mild processing steps makes it promising not only for the encapsulation of cellular cargo, but also to broader applications involving sensitive molecules, including proteins and RNAs.[51,52]

To prove our concept, the immiscible ATPS Dextran/PEG phases were used to mix oppositely charged polyelectrolytes. Despite the characteristic low interfacial tension of ATPS,[53] the drop-wise addition of the dispersed Dex+ALG phase into the continuous PEG+PLL phase, under agitation, led to the formation of single capsules with firm spherical morphology, showing that the interfacial tension and probable immediate initiation of interfacial complexation was enough to ensure that the system was kept stable, avoiding droplet's breakage. These characteristics allowed the adaptation of the system to the formation of miniaturized capsules with high production yield. This was achieved by using an electrospraying apparatus, which promoted the atomization of the Dex+ALG phase during its extrusion. The relatively low size polydispersion obtained after this process' optimization suggests that, for both macro and micro setups, the generation of the primary droplets immediately mediated the formation of capsules. The extreme difference in the viscosity of

both solutions, with Phase I (~15 Pa.s, at 0.01 s^{-1}) about 10-fold more viscous that Phase II (~2 Pa.s, at 0.01 s^{-1}, Figure S1), with a consistent difference kept along a range of applied shear rates, may also contribute to the stabilization of the dispersed droplets. In an effort to explore the versatility of the system, the switching of the dispersed/continuous character of each phase was attempted. However, probably due to the much lower density of the PEG+PLL phase, as well as due to the high viscosity of the Dex+ALG phase, the entrance of PEG+PLL droplets in the Dex+ALG solution was not successful, as the PEG+PLL droplets tended to float at the air/Dex+ALG interface, hampering the formation of stable structures. In the ALG and PLL-loaded phases, both polyelectrolytes can move freely in each solution and are able to partition to the contiguous aqueous phase at different extents, depending on their affinity. In fact, the control over polyelectrolytes' affinity towards different phases has been suggested as a way to control capsules' thickness and permeability properties.[20] Moreover, tailoring of the thickness of the capsule's membrane has been achieved by varying the polyelectrolytes' concentration. In a PAH/PSS system, capsules thickness increased almost linearly with the polyelectrolyte's concentration.[20] Here, the stability and robustness of the capsules was evaluated according to the systematic variation of both polyelectrolytes, as well as with the complexation times. Relevant aspects concerning the application of millimetric capsules in the context of cell encapsulation – including their ability to withstand handling with a spatula **(Figure S4)** and their resistance to contact with air - were visually inspected and systematically presented in a heatmap (Figure 2A). The effective formation of capsule-like structures and the achievement of robustness directly correlated with higher concentrations of the polyelectrolytes and seemed to be especially controlled by the alginate's concentration. In fact, the use of 1.5% ALG enabled obtaining robust structures for 20 minutes of complexation, even in combination with the lowest concentration of PLL (0.5%). An interesting observation relied on the faster formation of robust micrometric structures by electrohydrodynamic atomization, showcasing similar opacity to the optimized

macrocapsules, but in periods of complexation as short as 5 minutes. Although the in/outflux of polyelectrolytes should be, in a primary analysis, mainly mediated by their molecular weight and molar concentration gradients, other phenomena should be considered. Dutcher and Chen[54] stated that smaller sized droplets lead to a smaller diffusion boundary layer thickness, which reduces the diffusion time for polyelectrolytes to form the polymeric membrane in micrometric capsules. Furthermore, the curvature was also reported to have an impact on molecules' transport to the interface, as in millimetric droplets (diameter higher than 1 mm) the spherical interface is of such order that the radius→∞ and approximates to a planar surface, creating a similar diffusion length scale for both phases, in contrast with the curvature in micrometric droplets. These factors may enable the faster interfacial complexation in microcapsules, leading to a consequent quicker shape fixation.

The ability to achieve robust structures with low concentrations of PLL was used as a criterion to select the 1.5%ALG+0.5%PLL condition for cell encapsulation. High concentrations of PLL have been directly correlated to cytotoxic effects[37,38] due to its high charge density. The polycationic interaction with the negatively charged cell membrane induces the formation of nanoscale holes and may increase its permeability by phospholipases' activation.[55,56] This formulation of polyelectrolytes was also tested for different complexation time. We sought the decrease of processing time, so a rapid method could be developed, while protecting cells from interacting with possible unreacted PLL that could enter the Dex+ALG droplet during the complexation reaction. While for complexation times lower than 10 minutes only fragile structures could be obtained, 15 minutes of reaction led to the formation of robust structures. Compared to LbL assembly of PLL/ALG/chitosan in liquified capsules, which takes 12 assembly steps (10 minutes/step),[30] the structures described here outperform their robustness, with infrequent membrane rupture after exposure to rotational stimulus from 8 g up to 769 g, for 60 minutes. Compared to liquid-core capsules prepared by all-aqueous interfacial complexation, including structures prepared of synthetic

strong polyelectrolyte pairs (e.g., PDDA and PSS, shell thickness ~150 nm [25]) and weak polyelectrolytes (e.g., alginate and chitosan, shell thickness < 1 μm [27]), the macrocapsules characterized here show much higher thickness, measured in the order of hundreds of micrometers in the wet state. Importantly, to the best of our knowledge, this is also the first time that the robustness of liquid-core capsules fabricated by all-aqueous interfacial complexation is characterized and demonstrated.

Despite their robust behavior, capsules processed under the optimized condition targeting cell encapsulation permitted the fast diffusion of linear molecules (here, model dextran-FITC) with molecular weights up to 150 kDa. Such feature not only allows envisioning these capsules as drug delivery reservoirs, but also as cellular containers, where cells are amenable to be continuously oxygenated, capable of exchanging nutrient and metabolic waste, and also receiving (low-molecular weight) protein-mediated signals, including cytokines and even antibodies[57–60] from the capsules' surrounding environment. The combination of (i) mild processing technique, (ii) robustness, (iii) permeability to protein-sized molecules, and (iv) compatibility with co-encapsulation of cells and cell-adhesive microcarriers enabled envisioning this system as a promising platform for cellular encapsulation and long-term 3D culture, including in a bioreactor dynamic environment. In fact, the analysis of an early time point – 1 day after culture - showed that the encapsulation process displayed low cytotoxicity. Longer-term analysis up to 21 days (and 60 days for static culture, Figure S3) corroborated the adequacy of the system as a support for the expansion and culture of hUC-MSCs. Additionally, stirred tank culture led to rapid proliferation, in agreement with previous literature's reports that correlate shear stress and enhanced molecular exchange with faster cell expansion.[61–64] The adequacy of the developed capsules as supports for long-term cell culture up to 60 days was proved. Cellular adhesion to the capsules' walls was probably promoted by the presence of PLL in the biomaterial, previously reported as a promoter of cell adhesion.[65] Encapsulated cells forming multicellular/microcarriers aggregates caused the

rupture of the capsules' walls after adhesion, in events apparently led by the mechanical stretching of the capsules by these micro- to millimetric-sized cell-rich newly formed structures. Interestingly, the escape of these cellular aggregates from the capsule environment did not lead to the catastrophic breakage of the biomaterial structure. One may take advantage of this unusual phenomenon to design innovative time-morphing cellular systems that initially acts on the basis of paracrine-only contact and, by the sole action of encapsulated cells (in this case, their ability to rupture a biomaterial involucre), become cell-delivery vehicles.

4. Conclusion

In summary, we report the one-step fabrication of electrostatically complexed liquid-core robust capsules in mild and cytocompatible conditions. Millimetric capsules were prepared by a simple dropwise addition, and miniaturized structures were obtained by an electrohydrodynamic atomization methodology compatible with continuous production and high yield. The rapidly fabricated capsules showcased permeability and enabled the successful encapsulation of hUC-MSCs, with high clinical relevance, and their co-entrapment with polymeric cell-adhesive microcarriers. The preparation of these hierarchically organized structures enabled long-term culture of viable and proliferating hUC-MSCs, including in a stirred tank configuration. We demonstrated the possibility of processing multi-scale compartments with low quantity of biomaterials that could be used in bottom-up tissue engineering strategies.[66] These results establish a proof-of-concept for the use of compartmentalized microcarrier-laden capsules for the culture of adherent cells under biotechnologically relevant setups, including 3D dynamic culture. This newly described technology may find application in stem cell expansion and differentiation, as well as in a myriad of therapeutic purposes and biotechnological applications based on cell encapsulation.

5. Experimental Section

Experimental Design

The production of liquid-core capsules was based on the electrostatic complexation of two oppositely charged polymers at the interface of an aqueous two-phase system. The composition of each ATPS' phase followed the phase diagram reported elsewhere.[67] Two separate phases were prepared: (i) a dispersed phase - Phase I -, which consisted of Dextran Leuconostoc spp. (15% (w/w), Mw ~ 500 kDa, Sigma-Aldrich) mixed with alginate (1.5% (w/w), alginic acid sodium salt from brown algae, 71238-0250, Sigma-Aldrich) dissolved in Dulbecco's Phosphate-Buffered Saline (DPBS, Corning, pH 7.4), at room temperature (RT). For cell encapsulation experiments, the solution was dissolved in cell culture medium; (ii) a continuous phase - Phase II -, comprising poly(ethylene glycol) (17% (w/w), Mw ~ 8 kDa, Sigma-Aldrich) mixed with ε-poly-L-lysine (0.5% (w/w), Mw ~4.7 kDa, Epolyly® Pure, Handary S.A.) dissolved in DPBS, pH 7.4. The pH of both phases was adjusted after complete dissolution of the polyelectrolytes to pH 7.4 with 10 M NaOH.

Two methodologies were used to produce biocompatible capsules with distinct sizes: (i) 'macrocapsules' (millimetric-sized capsules) were fabricated by the dropwise addition of Phase I, using a 21G needle, to a stirring bath of Phase II, at 350 rpm. Complexation occurred for 15 minutes before 3 washing cycles with DPBS, under agitation; (ii) 'microcapsules' (micrometric-sized structures) were prepared using an electrohydrodynamic atomization (Spraybase, Avectas) equipment. Phase II was used as a collector bath and complexation occurred for 5 minutes. The operating parameters were a flow rate of 10 $mL.h^{-1}$, 22G needle, working distance (tip to collector distance) of 10 cm and 10 kV of voltage.

ζ-Potential's measurements

The ζ-potential of the phases with and without polyelectrolytes, freshly made or stored for one week at 4 ºC, was measured by Malvern Zetasizer Nano Zs equipment (Malvern Instruments

Ltd., Malvern, United Kingdom) at 25 °C. Each value was obtained in quadruplets as an average from three subsequent runs of the equipment with, at least, 10 measurements.

Rheological characterization of polyelectrolyte-loaded ATPS' phases

The response of both polyelectrolyte-loaded ATPS Phase I and Phase II to different shear rates was quantitatively assessed by a dynamic oscillatory rheology assay. The rheological measurements were collected by a Kinexus Pro+ Rheometer at room temperature, using a stainless-steel parallel plate geometry. Complex viscosity was recorded and analyzed.

Production and surface characterization of microcarriers

Poly(ε-caprolactone) (PCL) microparticles were produced by an emulsion solvent evaporation technique, as described elsewhere.[50] Briefly, a solution of PCL 80 kDa molecular weight (5% (w/v), Merck) in methylene chloride (Honeywell) was gradually added to a stirring solution of polyvinyl alcohol (0.5% (w/v), Merck), and left under agitation for 2 days at RT. A sieve was used to select microcarriers with diameters between 40 µm and 50 µm, which were thoroughly washed with distilled water, followed by 3 washing cycles with ethanol 100% (v/v) and dried overnight at RT. The surface of the microcarriers was first modified by ion coupled plasma treatment. Microparticles were placed inside a low-pressure plasma reactor chamber (Plasma System ATTO, electronic diener) and air was used as the working atmosphere to generate a glow discharge at 0.2-0.4 mbar, 30 V, for 15 minutes. The process was stopped every 5 minutes, so PCL microparticles were repositioned by shaking to improve the homogeneity of surface's modification. Following this process, microparticles were disinfected by an overnight immersion in 70% (v/v) ethanol at RT. After thoroughly washing with sterile DPBS, PCL microparticles were incubated in a solution of type I collagen (10 $\mu g.cm^{-2}$, collagen type I from rat protein tail, Sigma-Aldrich, prepared in 20 mM aqueous acetic acid solution (Chem-Lab NV)) for 4 hours, at 37 °C. The prepared microcarriers were

then washed 3 times with sterile DPBS to remove excess collagen and stored at 4 °C until encapsulation assays.

Evaluation of capsules' mechanical resistance

The resistance of macrocapsules to shear stress was evaluated using a rotational test. For each experimental condition, 10 capsules were placed in centrifuge tubes (in triplicates) containing DPBS (5 mL). The tubes were rotated at a speed of 8 g for 60 minutes. Every 15 minutes, the number of damaged capsules was counted by naked eye observation. An additional rotation cycle at 769 g for 15 minutes was performed and the number of damaged capsules was quantified.

Characterization of capsules' permeability's properties

Fluorescein isothiocyanate–dextrans (Dextran-FITC, Sigma-Aldrich) with different average molecular weights – 10kDa, 40 kDa, 70 kDa, 150 kDa, and 500 kDa - were mixed with Phase I at a concentration of 1 $mg.mL^{-1}$. Macrocapsules were prepared using the previously described method using this solution. For release studies, DPBS (5 mL) was added to 10 capsules, in triplicates, and incubated at 50 rpm at 37 °C. For every time point, 100 µL of the release medium was collected to a white opaque reading plate (Corning®) and 100 µL of fresh DPBS was added to the flask. Fluorescence was read at an excitation of 490 nm and an emission of 520 nm. Data are presented as the percentage of the released mass' cumulative overtime, considering a total loading efficiency of dextran-FITC's molecules (neglectable fluorescence values were detected on the Phase II solution retrieved after the preparation of capsules).

Macrocapsules' diameter's measurements

Macrocapsules' diameter was measured for a total of 70 capsules using ImageJ image analysis software (NIH, USA).

Macrocapsules' thickness' measurement

Macrocapsules' thickness was measured for a total of 25 capsules (5 from each of a total of 5 independent productions) using a digital micrometer.

Microcapsules' diameter's measurements

The size of microcapsules was measured by analysis of microscopy images using the ImageJ image analysis software. The determined average diameter corresponds to the measurement of a total of 30 microcapsules, 10 microcapsules from each of a total of 3 independent productions.

Morphological Analysis of Capsules

Capsules were dehydrated by immersion in a ethanol's concentration's gradient (30% (v/v), 50% (v/v), 70% (v/v), 80% (v/v), 90% (v/v), 96% (v/v) and 100% (v/v)) for 15 minute each and mounted on SEM supports using a double-sided carbon tape. Further gold sputtering was performed for 3 minutes. Scanning Electron Microscopy (SEM, Hitachi, SU-70 instrument) was used at an accelerating voltage of 8 kV.

Preparation of Hierarchical Structures: Microcapsules encapsulated in Macrocapsules

Microcapsules were prepared by EHDA using a collector bath of PEG (17% (w/w)) and PLL (0.5% (w/w)) in DPBS, under agitation, and a dispersed phase of dextran (15% (w/w)) and alginate (0.90% (w/w)) in DPBS. The operating parameters used were a flow rate of 10 $mL.h^{-1}$, 24G needle, working distance of 10 cm and 10 kV of voltage. The complexation occurred for 5 minutes. These micro-sized structures were thoroughly washed with DPBS and

resuspended in Phase I (15% (w/w) dextran and 1.5% (w/w) alginate in DPBS) for the macrocapsules production following the previously described procedure.

Cell isolation and characterization

L929 (European Collection of Authenticated Cell Cultures) were culture in DMEM low-glucose (Dulbecco's modified Eagle medium, Sigma-Aldrich), supplemented with heat-inactivated FBS (10% (v/v)) and penicillin−streptomycin (1% (v/v)), at pH 7.4. Cells were grown in 175 cm^2 adherent tissue culture flasks and incubated at 37 °C in a humidified air atmosphere of 5% CO_2. Every three days, fresh medium was added.

Umbilical cords (UCs) were obtained from healthy women who underwent infant delivery, either by C-section or vaginal birth, and after signing the informed consent. The collected tissues were obtained under a cooperation agreement between COMPASS Research Group from CICECO-University of Aveiro and Aveiro local hospital Centro Hospitalar do Baixo Vouga, after approval of the hospital Ethics Committee (EC). The UCs were transported to the laboratory facilities in phosphate-buffered saline (PBS, ThermoFisher Scientific) supplemented with penicillin-streptomycin (10% (v/v), ThermoFisher Scientific) and handled according to guidelines approved by the EC. Samples were processed under sterile conditions within 24 hours after delivery. MSCs were isolated from the Wharton's jelly (MSCs-WJ) using the explant method. For that, the UC was washed with sterile PBS to remove blood and blood clots, and subsequently cut into small pieces of ca. 3 cm. After removal of the vein and two arteries, small pieces of the WJ were transferred to cell adhesive petri-dishes. The tissues explants were incubated at 37 ºC in a humidified atmosphere of 5% of carbon dioxide for 2 hours. Minimum Essential Medium Alpha (α-MEM) supplemented with antibiotic-antimycotic (1% (v/v), ThermoFisher Scientific) and heat-inactivated fetal bovine serum (10% (v/v), ThermoFisher Scientific) was added until immersion of the tissue pieces, following incubation at 37 ºC and 5% of CO_2. After cell migration, the tissue explants were

removed from the petri-dish. At 90% confluence, WJ-MSCs were detached using trypsin-EDTA solution (ThermoFisher Scientific) and expanded at a density of $5x10^3$ cells per cm^2. Afterwards, the successful isolation of WJ-MSCs was characterized by flow cytometry (BD Accuri C6 Plus). At 90% confluence, WJ-MSCs were detached (TrypLETM Express, ThermoFisher Scientific) and resuspended in DPBS containing bovine serum albumin (2% (w/v), Merk) and sodium azide (0.1% (v/v), TCI). Cells were then incubated with CD73 (PE-conjugated, Biolegend), CD90 (AlexaFluor 647-conjugated), CD34 (FITC-conjugated) and CD31 (APC-conjugated) antibodies according to manufacturer's specifications (Biolegend). After 45 minutes at RT, samples were washed in DPBS, and resuspended in DPBS containing formaldehyde (1% (v/v), Sigma-Aldrich) and sodium azide (0.1% (w/v)) for analysis. Flow cytometry results confirmed the successful isolation of a population of MSCs highly expressing the stemness markers CD 90 (92.3%) and CD 73 (93.4%), whilst lacking the hematopoietic and endothelial markers CD 34 (0.4%) and CD 31 (2.1%), respectively.

Cell Encapsulation

The ATPS' phases, without added polyelectrolytes, were filtrated with a 0.2 µm sterile filter (Whatman® Puradisc Ø30mm, Zmed). ALG and PLL powder were exposed to UV radiation for 40 minutes. The process was stopped after 20 minutes and both polyelectrolytes were repositioned by shaking to improve the homogeneity of sterilization. Afterwards, they were respectively added to each ATPS' phase, at the previously described concentrations. Sterilized surface-functionalized PCL microcarriers were then added at a concentration of 30 $mg.mL^{-1}$ to Phase I and resuspended using a micropipette. hUC-MSCs (passage 4) at 90% of confluence were washed with DPBS and chemically detached using trypsin-EDTA solution (Merck) for 5 minutes, at 37 °C. hUC-MSCs were suspended in Phase I with PCL microcarriers at a cell density of 5×10^6 $cells.mL^{-1}$. Macrocapsules were then processed using the aforementioned method. After complexation, excess of Phase II was removed by 3

washing steps (5 minutes each) using sterile DPBS. Cell-laden macrocapsules were cultured in supplemented α-MEM medium, in well-plates (static condition) or in a spinner flask at 50 rpm (Celstir, Wheaton). For static culture, 4 capsules were cultured in 1 mL of supplemented α-MEM medium, in triplicates for each time point. For dynamic assays, a total of 72 capsules were added to 75 mL of supplemented α-MEM medium. Both assays were conducted for 21 days, in a humidified 5% CO_2 air atmosphere, at 37 °C. Cell culture medium was replenished every 2 days.

The preparation of solutions for EHDA processing followed the same procedure as the ones used for macrocapsules. The equipment's operating parameters were set for a flow rate of 10 $mL.h^{-1}$, 22G needle with blunt end, working distance (tip of the needle-collector) of 10 cm, and 10 kV voltage. Cell-laden microcapsules were cultured in static complete α-MEM medium, in a well-plate for 14 days, in a humidified 5% CO_2 air atmosphere, at 37 °C. Cell culture medium was replenished every 2 days.

Metabolic Activity and Cell's Viability of Encapsulated Cells

Cell viability in the macro- and microcapsules was evaluated using the live-dead fluorescence assay (ThermoFisher Scientific). Samples were incubated in DPBS solution (1 mL) containing calcein AM (2 µL, 2 $\mu g.mL^{-1}$; Thermo Fisher Scientific) and propidium iodide (PI; 1 µL, 1 $ug.mL^{-1}$; Thermo Fisher Scientific), at 37 ºC, for 10 minutes. Encapsulated cells were washed 3 times with sterile DPBS and visualized by fluorescence microscopy (Axio Imager 2, Zeiss) after 1, 3, 7, 14 and 21 days of culture.

The metabolic activity of encapsulated hUC-MSCs was assessed by the CellTiter 96® AQueous One Solution Cell Proliferation Assay (MTS, 3-[4,5,dimethylthiazol-2-yl]-5-[3-carboxymethoxy-phenyl]-2-[4- sulfophenyl]-2H-tetrazolium, inner salt, Promega, USA). After 1, 3, 7, 14 and 21 days in culture, 4 capsules in triplicates were incubated for 4 hours, at 37 °C in a humidified air atmosphere of 5% CO_2. For each timepoint, 100 µL of each well (in

triplicate) was transferred to a 96-well plate and measured by absorbance at a wavelength of 490 nm using a spectrophotometer (Gen 5 2.01, Synergy HTX, Bio-TEK).

Assessment of Cellular Organization and Morphology

For the spatial organization of encapsulated cells, phalloidin red (5:200 in PBS, Biolegend) and 4',6-diamidino-2-phenylindole dihydrochloride (DAPI, 1:1000, 1 mg.mL−1 in DPBS, Thermo- Fisher Scientific) were used to display the F-actin distribution in cell's cytoskeleton and their nuclei, respectively. Capsules in culture for 1, 3, 7, 14 and 21 days were washed with DPBS, fixed with formalin (4% (v/v)), for 2 hours, at RT, and permeabilized for 5 minutes with Triton-X (0.1% (v/v), Merck) at RT. Samples were then incubated with phalloidin red for 45 minutes, at 37 °C, washed with DPBS, and finally stained with DAPI for 5 minutes, at RT. The structures were analyzed by fluorescence microscopy (Axio Imager 2, Zeiss).

DNA quantification

Macrocapsules cultured for 21 days were analyzed for their DNA amount in each studied timepoint. To promote cellular lysis and extract dsDNA, four capsules per time-point, in triplicates, were immersed in ultra-pure water with Triton-X (0.2% (v/v)) and incubated for 1 hour at 37 ºC. Afterwards, samples were frozen at -20 ºC and kept stored until quantification, following manufacturer's specifications (Quant-iT™ PicoGreen® dsDNA assay kit, Thermo Fisher Scientific). To plot a standard curve, a solution of a λDNA standard provided by the manufacturer was used. After 10 minutes of incubation at RT, fluorescence was read at an excitation wavelength of 485/20 nm and an emission of 528/20 nm, using a microplate reader.

Statistical Analysis

All data was expressed as mean ± standard deviation. Two-way ANOVA test with multiple comparison test was applied to identify significant differences between static and dynamic conditions for the biological assays. A p-value <0.05 was considered statistically significant using GraphPad Prism 6.0 software. MTS for cell metabolic activity analysis and DNA quantification results were grouped by timepoint, for static and dynamic environment, respectively, to analyze significant differences between conditions.

Supporting Information
Supporting Information is available from the Wiley Online Library or from the author.

Acknowledgements
This work was supported by the European Research Council grant agreement ERC-2014-ADG-669858 for project "ATLAS". It was developed within the scope of the project CICECO-Aveiro Institute of Materials, UIDB/50011/2020 & UIDP/50011/2020, financed by national funds through the FCT/MEC and when appropriate co-financed by FEDER under the PT2020 Partnership Agreement. The authors disclaim do not have any conflict of interests.

Received: ((will be filled in by the editorial staff))
Revised: ((will be filled in by the editorial staff))
Published online: ((will be filled in by the editorial staff))

[1] C. R. Correia, R. L. Reis, J. F. Mano, *Adv. Healthc. Mater.* **2018**, *7*, 1.

[2] T. Nonoyama, J. P. Gong, *Proc IMechE Part H J Eng. Med.* **2015**, *229*, 853.

[3] R. Dembczynski, T. Jankowski, *Biochem. Eng. J.* **2000**, *6*, 41.

[4] F. Lim, A. M. Sun, *Science (80-.).* **1980**, *210*, 908.

[5] C. S. Peyratout, L. Dähne, *Angew. Chem. Int. Ed.* **2004**, *43*, 3762.

[6] G. Duan, M. F. Haase, K. J. Stebe, D. Lee, *Langmuir* **2018**, *34*, 847.

[7] J. A. Burdick, S. J. Yeo, P. J. Yoo, M. Kim, J. Doh, D. Lee, C. B. Highley, *ACS Nano* **2015**, *9*, 8269.

[8] A. P. R. Johnston, C. Cortez, A. S. Angelatos, F. Caruso, *Curr. Opin. Colloid Interface Sci.* **2006**, *11*, 203.

[9] Z. Yang, B. Xu, *Adv. Mater.* **2006**, *18*, 3043.

[10] W. Tong, X. Song, C. Gao, *R. Soc. Chem.* **2012**, *41*, 6103.

[11] A. L. Becker, A. P. R. Johnston, F. Caruso, *Macromol. Biosci.* **2010**, *10*, 488.

[12] C. R. Correia, T. C. Santos, R. P. Pirraco, M. T. Cerqueira, A. P. Marques, R. L. Reis, J. F. Mano, *Acta Biomater.* **2017**, *53*, 483.

[13] A. E. May, E. L. Tilokee, N. Latham, B. Mcneill, B. Lam, M. Ruel, E. J. Suuronen, D. W. Courtman, D. J. Stewart, D. R. Davis, *Biomaterials* **2014**, *35*, 133.

[14] F. Kang, G. Jiang, A. Hinderliter, P. P. Deluca, J. Singh, *Pharm. Res.* **2002**, *19*, 629.

[15] H. Cheung, *J. Mater. Chem. B.* **2016**, *4*, 1213.

[16] P. A. Albertsson, *Wiley, New York* **1986**, *3*.

[17] C. M. S. S. Neves, S. Shahriari, J. Lemus, J. F. B. Pereira, M. G. Freire, J. A. P. Coutinho, *Phys. Chem. Chem. Phys.* **2016**, *18*, 20571.

[18] Y. Chao, H. C. Shum, *Chem. Soc. Rev.* **2020**, *49*, 114.

[19] S. D. Hann, K. J. Stebe, D. Lee, *ACS Appl. Mater. Interfaces* **2017**, *9*, 25023.

[20] Q. Ma, Y. Song, J. W. Kim, H. S. Choi, H. C. Shum, *ACS Macro Lett.* **2016**, *5*, 666.

[21] H. Cheung Shum, J. Varnell, D. A. Weitz, *Biomicrofluidics* **2012**, *6*, 1.

[22] S. Hardt, T. Hahn, *Lab Chip* **2012**, *12*, 434.

[23] S. D. Hann, D. Lee, K. J. Stebe, *Phys. Chem. Chem. Phys.* **2017**, *19*, 23825.

[24] Y. Song, Y. K. Chan, Q. Ma, Z. Liu, H. C. Shum, *ACS Appl. Mater. Interfaces* **2015**, *7*, 13925.

[25] L. Zhang, L. H. Cai, P. S. Lienemann, T. Rossow, I. Polenz, Q. Vallmajo-Martin, M. Ehrbar, H. Na, D. J. Mooney, D. A. Weitz, *Angew. Chem.* **2016**, 128, 13668– 13672; *Angew. Chemie - Int. Ed.* **2016**, *55*, 13470-13474.

[26] S. D. Hann, T. H. R. Niepa, K. J. Stebe, D. Lee, *ACS Appl. Mater. Interfaces* **2016**, *8*, 25603.

[27] H. Liu, Y. Wang, H. Wang, M. Zhao, T. Tao, X. Zhang, J. Qin, *Adv. Sci.* **2020**, 1.

[28] C. Bellotti, S. Duchi, A. Bevilacqua, E. Lucarelli, F. Piccinini, *Cytotechnology* **2016**,

68, 2479.

[29] S. Lee, E. Choi, M. Cha, K. Hwang, *Oxid. Med. Cell. Longev.* **2015**, *2015*, 1.

[30] C. R. Correia, R. L. Reis, J. F. Mano, *Biomacromolecules* **2013**, *14*, 743.

[31] C. R. Correia, P. Sher, R. L. Reis, J. F. Mano, *Soft Matter* **2013**, *9*, 2125.

[32] A. Grotzky, Y. Manaka, S. Fornera, M. Willeke, P. Walde, *Anal. Methods* **2010**, *2*, 1448.

[33] K. I. Draget, G. Skjåk Bræk, O. Smidsrød, *Carbohydr. Polym.* **1994**, *25*, 31.

[34] E. Diamanti, N. Muzzio, D. Gregurec, J. Irigoyen, M. Pasquale, O. Azzaroni, M. Brinkmann, S. E. Moya, *Colloids Surfaces B Biointerfaces* **2016**, *145*, 328.

[35] M. Rimann, T. Lühmann, M. Textor, B. Guerino, J. Ogier, H. Hall, *Bioconjugate Chem.* **2008**, *19*, 548.

[36] H. J. Griesser, N. D. Spencer, M. Textor, *J. Phys. Chem. B* **2005**, *109*, 17545.

[37] Z. Kadlecova, L. Baldi, D. Hacker, F. M. Wurm, H. A. Klok, *Biomacromolecules* **2012**, *13*, 3127.

[38] D. Fischer, Y. Li, B. Ahlemeyer, J. Krieglstein, T. Kissel, *Biomaterials* **2003**, *24*, 1121.

[39] M. J. York-Duran, M. Godoy-Gallardo, C. Labay, A. J. Urquhart, T. L. Andresen, L. Hosta-Rigau, *Colloids Surfaces B Biointerfaces* **2017**, *152*, 199.

[40] K. M. Kim, J. Kim, *J. Mater. Sci. Mater. Med.* **2012**, *23*, 753.

[41] M. Schmid-schwap, A. Franz, F. König, M. Bristela, T. Lucas, E. Piehslinger, D. C. Watts, A. Schedle, *Dent. Mater.* **2009**, *25*, 360.

[42] International Standards Organization (ISO) 10993-5: Biological evaluation of medical devices - part 5. Geneva, Switzerland. **2009**.

[43] R. P. H. Meier, R. Mahou, P. Morel, J. Meyer, E. Montanari, Y. D. Muller, P. Christofilopoulos, C. Wandrey, C. Gonelle-gispert, L. H. Bühler, *J. Hepatol.* **2015**, *62*, 634.

[44] A. Moshaverinia, S. Ansari, C. Chen, X. Xu, K. Akiyama, M. L. Snead, H. H. Zadeh,

S. Shi, *Biomaterials* **2013**, *34*, 6572.

[45] A. S. Magin, N. R. Körfer, H. Partenheimer, C. Lange, A. Zander, T. Noll, *Stem Cells Dev.* **2009**, *18*.

[46] H. Motaln, C. Schichor, T. T. Lah, *Cancer* **2010**, *116*, 2519.

[47] P. Moretti, T. Hatlapatka, D. Marten, A. Lavrentieva, I. Majore, R. Hass, C. Kasper, *Adv Biochem Eng Biotechnol.* **2010**, *123*, 29.

[48] Y. Li, G. Guo, L. Li, F. Chen, J. Bao, Y. Shi, *Cell Tissue Res.* **2015**, *360*, 297.

[49] D. Chen, H. Hao, C. Tong, J. Liu, L. Dong, D. Ti, Q. Hou, H. Liu, *Int. J. Low. Extrem. Wounds* **2015**.

[50] S. Nadine, S. G. Patrício, C. R. Correia, J. F. Mano, *Biofabrication* **2020**, *12*, 1.

[51] H. Zhang, Y. Wang, Y. Zhou, K. Xu, N. Li, Q. Wen, Q. Yang, *Talanta* **2017**, *170*, 266.

[52] R. J. Meagher, Y. K. Light, A. K. Singh, *Lab Chip* **2008**, *8*, 527.

[53] J. Ryden, P.-A. Albertsson, *J. Colloid Interface Sci.* **1971**, *37*, 219.

[54] Y. Chen, C. S. Dutcher, *Soft Matter* **2020**, *16*, 2994.

[55] W. Zauner, M. Ogris, E. Wagner, *Adv. Drug Deliv. Rev.* **1998**, *30*, 97.

[56] S. Hong, P. R. Leroueil, E. K. Janus, J. L. Peters, M. Kober, M. T. Islam, B. G. Orr, J. R. Baker, M. M. B. Holl, *Bioconjugate Chem.* **2006**, *17*, 728.

[57] A. Kelso, *Curr. Opin. Immunol.* **1989**, *2*, 215.

[58] D. Flaherty, In *Immunology for Pharmacy*; 2012; pp. 70–78.

[59] J. A. Stenken, A. J. Poschenrieder, *Anal. Chim. Acta* **2015**, *853*, 95.

[60] T. W. Mak, M. E. Saunders, In *The Immune Response*; 2006; pp. 93–120.

[61] G. Eibes, P. Z. Andrade, J. S. Boura, M. M. A. Abecasis, C. Lobato, J. M. S. Cabral, **2010**, *146*, 194.

[62] F. Santos, A. Campbell, A. Fernandes-platzgummer, P. Z. Andrade, J. M. Gimble, Y. Wen, S. Boucher, *Biotechnol. Bioeng.* **2014**, *111*, 1116.

[63] F. Petry, J. R. Smith, J. Leber, D. Salzig, P. Czermak, M. L. Weiss, *Stem Cells Int.*

2016, *2016*, 1.

[64] Y. Yu, K. Li, C. Bao, T. Liu, *Appl Biochem Biotechnol* **2009**, *159*, 110.

[65] G. Rainaldi, A. Calcabrini, M. T. Santini, *J. Mater. Sci. Mater. Med.* **1998**, *9*, 755.

[66] V. M. Gaspar, P. Lavrador, J. Borges, M. B. Oliveira, J. F. Mano, *Adv. Mater.* **2020**, *32*, 1.

[67] A. Sauret, H. C. Shum, *Appl. Phys. Lett.* **2012**, *100*, 1.

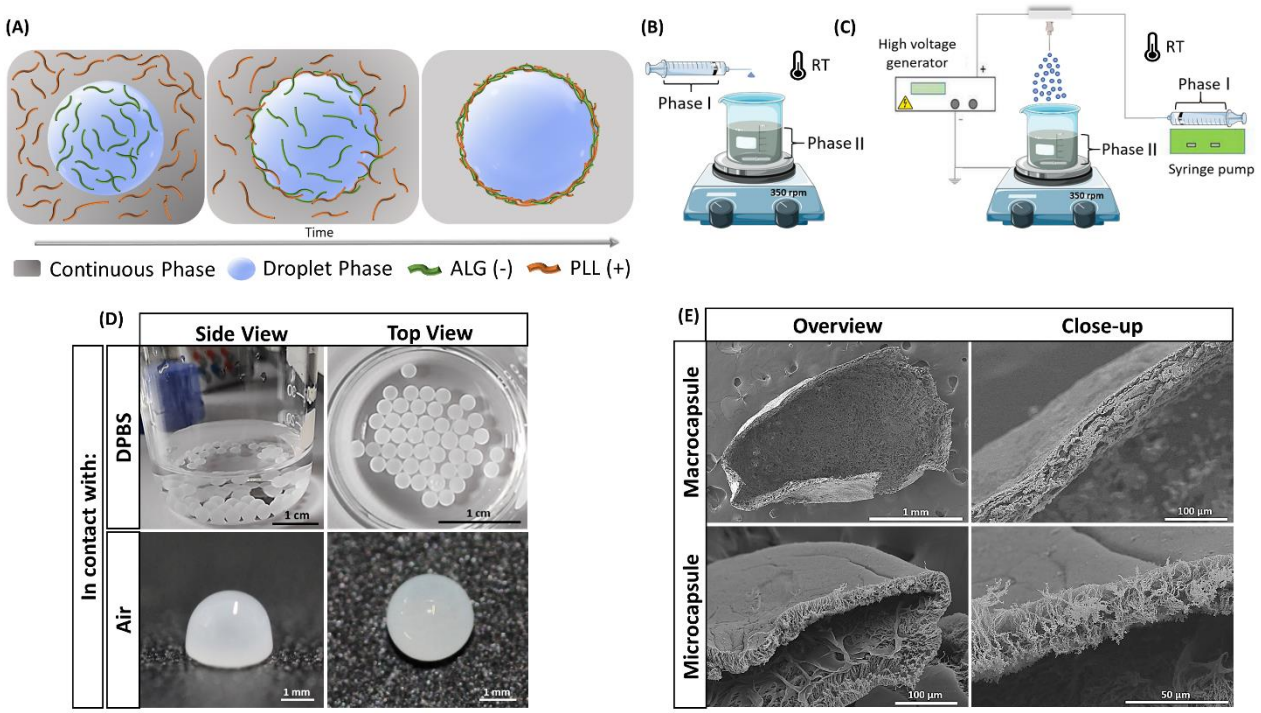

Figure 1. Production and characterization of macro and microcapsules assembled at the ATPS interface. **(A)** Schematic representation of the complexation of alginate (ALG) and ε-poly-L-lysine (PLL) at the interface of the aqueous immiscible interface, leading to the formation of capsules. **(B)** Schematic representation of the production of macrocapsules by dropwise addition of Phase I into Phase II, under agitation. **(C)** Schematic representation of the production of microcapsules by electrohydrodynamic atomization of Phase I into Phase II, under agitation. **(D)** Photographs of macrocapsules (produced by dropwise addition) and their opaque robust interfacial membrane immersed in DPBS, a phosphate-buffered saline solution, (top), or placed on a dry surface exposed to air (bottom).The photographs show the stability of the capsules, either when wet or exposed to dry environments, showcasing the robustness of the system. **(E)** SEM images of macro- and microcapsules with respective cross-sections, displaying the morphology and structure of the membrane.

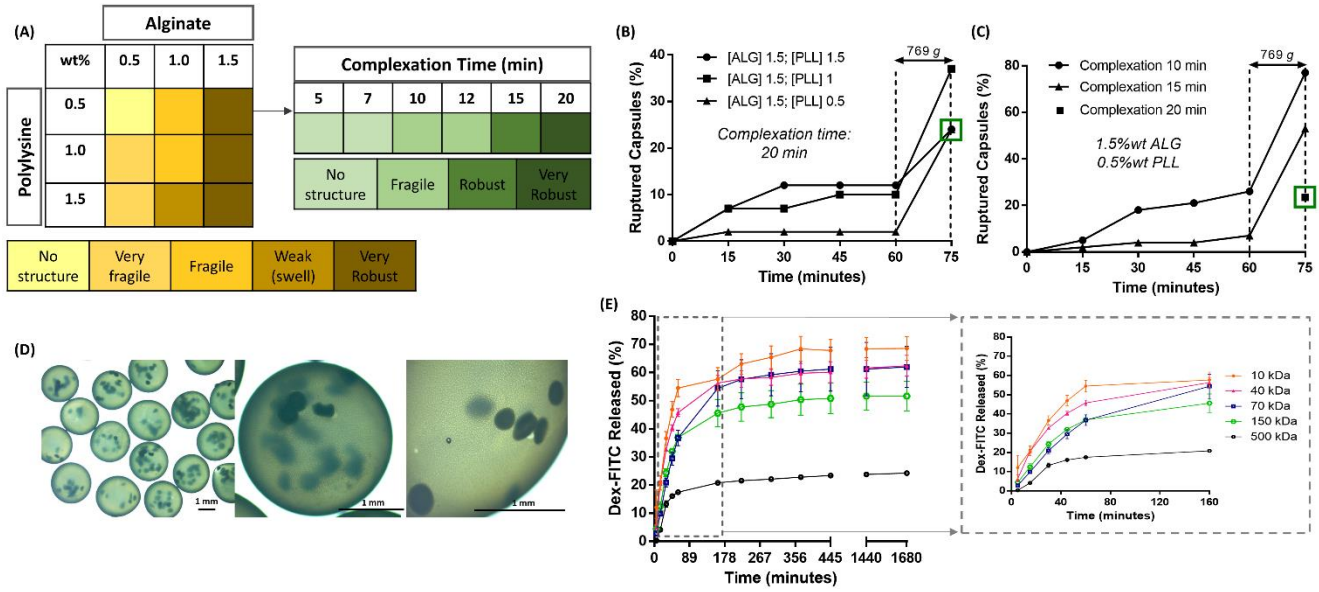

Figure 1. Mechanical features of macrocapsules and characterization of the permeability. **(A)** Qualitative characterization of macrocapsules' robustness processed with different polyelectrolyte concentrations and a complexation time of 20 minutes (yellow color gradient diagram), and complexation times for [ALG],[PLL]wt% = 1.5%, 0.5% (green color gradient diagram). **(B)** Assessment of macrocapsules' robustness by a rotational test regarding polyelectrolytes' concentration. **(C)** Assessment of macrocapsules' robustness by a rotational test regarding complexation time for [ALG],[PLL]wt% = 1.5%, 0.5%. **(D)** Encapsulation of micro- in macro-capsules, generating multi-compartmentalized structures. **(E)** Release of dextran-FITC model molecules from macrocapsules over 28 hours (results presented as means ± SD). The inset represents the first 160 minutes of dextran-FITC release, when a plateau phase is reached.

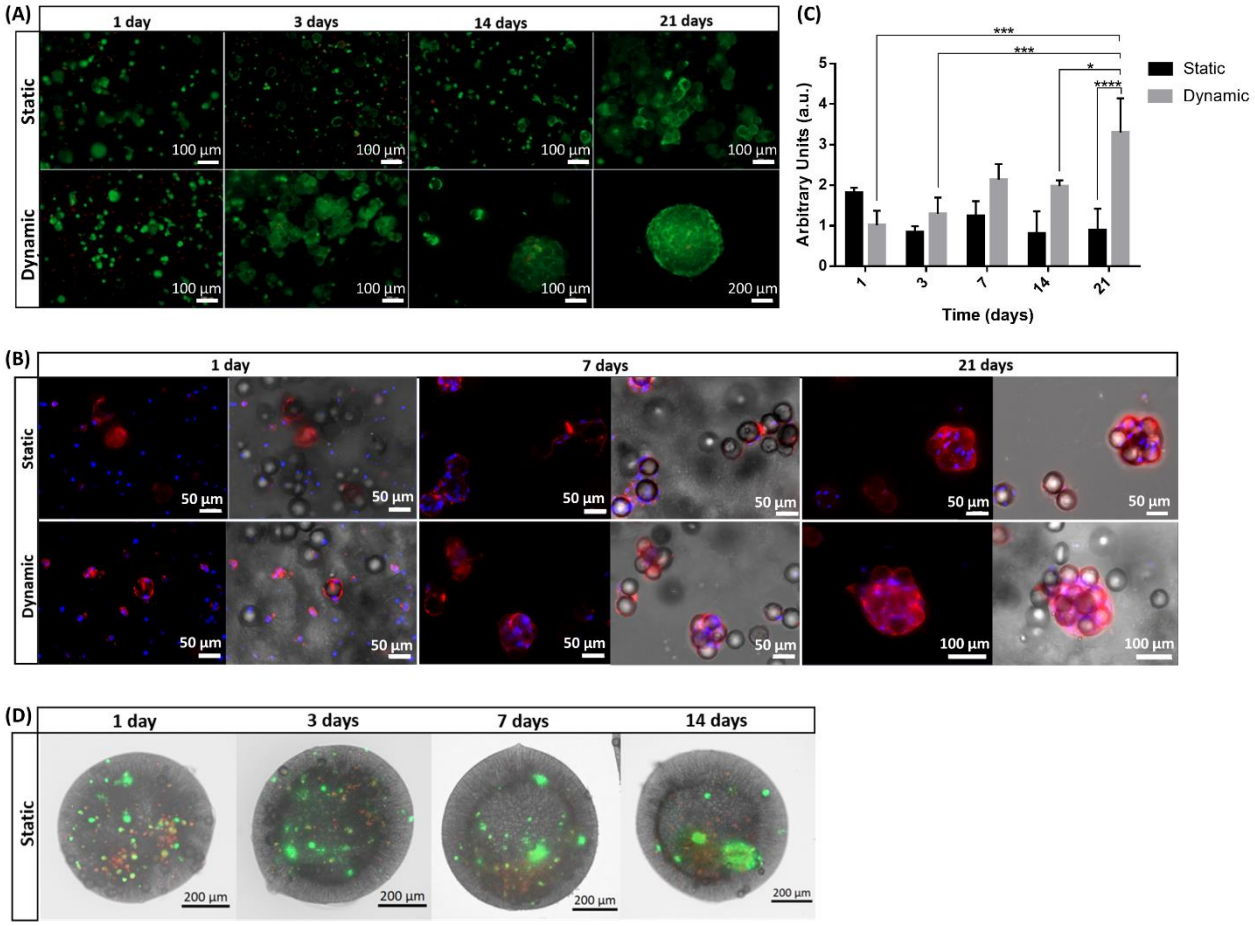

Figure 2. Viability and spatial organization of hUC-MSCs encapsulated in macro and microcapsules containing PCL microcarriers. **(A)** Live-dead assay for static and dynamic cell cultures. Living cells are stained in green, whereas dead cells are stained in red. **(B)** DAPI/Phalloidin staining was performed to assess cellular spatial organization inside the capsules. Cells adhered to PCL microparticles in both static and dynamic environments 1 day after encapsulation. In purple, DAPI stains the nuclei (in blue), and in red phalloidin marks the cytoskeleton's F-actin filament. Bright field images are also provided. **(C)** Metabolic activity evaluation by MTS colorimetric assay for 1, 3, 7, 14 and 21 days in culture (results presented as means ± SD), normalized by the quantification of dsDNA. **(D)** Live-dead assay on microcapsules laden with hUC-MSCs and PCL microcarriers for 1, 3, 7 and 14 days in culture.

Table of Contents

Robust polymeric capsules were produced using a one-step rapid process based on the interfacial complexation of oppositely charged polyelectrolytes in an all-aqueous environment. Two processing methodologies were used to produce millimetric or micrometric capsules and characterized regarding their size dispersity, thickness, robustness and porosity. Animal cells were successfully co-encapsulated with microcarriers as cell-adhesion sites, under static or dynamic condition, for 21 days.

Keyword: all-aqueous cell encapsulation

Sara Vilabril, Sara Nadine, Catarina M. S. S. Neves, Clara R. Correia, Mara G. Freire, João A. P. Coutinho, Mariana B. Oliveira*, João F. Mano*

One-step All-aqueous Interfacial Assembly of Robust Membranes for Long-term Encapsulation and Culture of Adherent Stem/Stromal Cells